Egyptian Journal of Aquatic Research 50 (2024) 566–576

Contents lists available at ScienceDirect

Egyptian Journal of Aquatic Research

journal homepage: www.elsevier.com/locate/ejar

Full length article

Immune cells in the spiral intestine of Blackmouth catshark, *Galeus melastomus*: New insights into ancient gut defenders

Giampaolo Bosi [a], Bahram Sayyaf Dezfuli [b], Paolo Merella [c], Luisa Giari [d,*]

[a] Department of Veterinary Medicine and Animal Science, University of Milan, dell'Università St. 6, 26900 Lodi, Italy
[b] Department of Life Sciences and Biotechnology, University of Ferrara, Borsari St. 46, 44121 Ferrara, Italy
[c] Department of Veterinary Medicine, University of Sassari, Vienna St. 2, 07100 Sassari, Italy
[d] Department of Environmental and Prevention Sciences, University of Ferrara, Borsari St. 46, 44121 Ferrara, Italy

ARTICLE INFO

Keywords:
Spiral intestine
Immune system
Elasmobranch
Immunohistochemistry
Confocal microscope

ABSTRACT

This study aimed to describe the morphology and to characterize the immunohistochemistry of the gut-associated lymphoid tissue (GALT) in the spiral intestine of the Blackmouth catshark *Galeus melastomus*. In the catshark, the lympho-myeloid aggregate of the GALT was mainly confined to the central region of the spiral valve. A panel of eight immune molecular markers was applied to histological sections to show the cell types of the GALT using immunohistochemical and -fluorescence methods. Two main reactive cell types were identified: (i) a mast cell lineage positive to histamine, serotonin, and immunoglobulin E-like receptor antibodies, and (ii) a macrophage lineage positive to CD4, interleukin-6, lysozyme, toll-like receptor-2, and tumor necrosis factor-α antibodies. Confocal microscopy revealed which immune markers were co-localized in the same cell type. The presence of cells positive to the tested antibodies confirmed the defensive role against pathogens of the GALT in the spiral intestine of the catshark. Given the limited knowledge of the elasmobranch immune system, the current study provides new insights into the features of ancient defender cells of the spiral intestine.

Introduction

Cartilaginous fish are the first vertebrates with true lymphoid organs (Zapata et al., 1996), among which elasmobranchs are the most primitive group containing immunoglobulin (Mitchell & Criscitiello, 2020). Sharks and rays lack bone marrow, so the spleen and the head kidney are the main sites of erythrocyte production, and the thymus is responsible for T cell proliferation. Meanwhile, Leydig's organ, located in the esophagus, and the epigonal organ, located on the outer region of the gonads, are the sites of granulocyte formation and B cell maturation (Mitchell & Criscitiello, 2020; Zapata et al., 1996).

In all fish, a secondary immune tissue is associated with the skin, gills, and gut. In the former, this tissue is located in the intestinal wall, precisely in the lamina propria, and is called gut-associated lymphoid tissue (GALT) (Mitchell & Criscitiello, 2020; Zapata et al., 1996). In elasmobranchs, the GALT is mainly located in the spiral intestine, a peculiar intestinal region with an internal helicoidal fold that increases the surface area for better nutrient uptake (Bosi et al., 2022; Mitchell & Criscitiello, 2020). The GALT in the spiral intestine is considered a primitive structure and ancestor of Peyer's patches in mammals (Mitchell & Criscitiello, 2020; Zapata & Amemiya, 2000). Notwithstanding, the immune cell aggregates of GALT are not a true lymphoid organ because they lack a connective capsule like Peyer's patches (Mitchell & Criscitiello, 2020; Zapata & Amemiya, 2000). The GALT consists of a large accumulation of cells in the lamina propria as well as individual cells scattered in the lamina propria and the epithelium (Hart et al., 1987). Compared with the plethora of studies on the GALT of teleosts, studies on the GALT of elasmobranchs are scarce and primarily focused on the morphological aspects (Smith et al., 2019). In the second half of the last century, several studies have been conducted on the ultrastructure of the leukocytes in the blood and the spiral intestine of some species of sharks and dogfish (Hart et al., 1987; Zapata et al., 1996). Based on ultrastructural features, Hart et al. (1987) identified five cell types in the spiral intestine of *Scyliorhinus canicula*, the small-spotted catfish: lymphocytes, plasma cells, and three types of granulocytes. Due to the high variability in the immune cells present in the spiral intestine of elasmobranchs, the morphological characteristics are still not well-known (Mitchell & Criscitiello, 2020).

There are different leukocyte classifications in elasmobranchs due to a lack of univocal criteria (Carmezim & Marcos, 2020; Hine & Wain,

* Corresponding author.
E-mail addresses: giampaolo.bosi@unimi.it (G. Bosi), dzb@unife.it (B. Sayyaf Dezfuli), paolomerella@uniss.it (P. Merella), grilsu@unife.it (L. Giari).

https://doi.org/10.1016/j.ejar.2024.10.002
Received 18 March 2024; Received in revised form 10 September 2024; Accepted 5 October 2024
Available online 2 November 2024

1987). There are few immunohistochemical studies differentiating the immune cells of shark and ray intestines (Anandhakumar et al., 2012; Lauriano et al., 2019; Sayyaf Dezfuli et al., 2018a). *Galeus melastomus*, the Blackmouth catshark, is a deep-sea species widespread in the Mediterranean Sea (Farrag, 2016). This study aimed to carry out the morphological characterization of the GALT cell types in the spiral intestine of *G. melastomus* using immunohistochemistry assays. A panel of eight antibodies against immune molecular markers already used in teleosts (Bosi et al., 2015; Da'as et al., 2011; Mulero et al., 2007; Sayyaf Dezfuli et al., 2018b, 2023a) and elasmobranchs (Sayyaf Dezfuli et al., 2018b, 2019) was chosen. Double-immunofluorescence reactions with a confocal microscope provided additional information on the co-localization of the used antibodies in the immune cells of the catshark spiral intestine.

Materials and methods

Animals

Fourteen specimens of the *G. melastomus* (five males and nine females) were provided on two occasions (January and April 2023) via commercial trawl fishing during a haul at a 500–800 m depth in the Gulf of Asinara (Sardinia, western Mediterranean Sea). Fish ranging from 165 to 274 g in wet weight (mean total length ± standard deviation: 42.6 ± 5.1 cm) were eviscerated, and the entire digestive tube of each was promptly fixed in 10 % neutral-buffered formalin while still on board. After landing, the samples were transported to the Department of Veterinary Medicine of the University of Sassari and processed within 24 h post-fixation. The spiral intestine of each specimen was sliced into small pieces, rinsed several times with chilled 70 % ethanol, and sent to the University of Ferrara for the embedding process in paraffin wax.

Histology and histochemistry

The fixed tissues were dehydrated via an alcohol series and then paraffin-wax-embedded using a Shandon Citadel 2000 Tissue Processor (Shandon, UK). Transverse serial sections of 5 μm thick were obtained, and slides were stained with hematoxylin and eosin (H&E), Giemsa, and Sirius Red and photographed using a Nikon Microscope ECLIPSE 80i (Nikon, Tokyo, Japan).

Immunohistochemistry

Several sections were sent to the University of Milan for the immunohistochemical (IHC) tests. Eight antibodies routinely used for the identification of innate immune cells in teleosts were applied to sections of the spiral intestine (Supplementary Table S1). Sections were rehydrated and rinsed in Tris-buffered saline at pH 7.6 (TBS: 0.05 M Tris-HCl; 0.15 M NaCl). The immunohistochemical protocol was the same as that reported in (Sayyaf Dezfuli et al., 2018a). The antigen retrieval procedure, consisting of heating sections for 2 × 5 min in a microwave at 500 W in a 0.01 M citrate buffer (pH 6.0), was performed for the rabbit polyclonal anti-cluster of differentiation 4 (CD4) and the rabbit polyclonal anti-tumor necrosis factor-α (TNF-α) antibodies (Supplementary Table S1). Controls were performed via (1) incubation with phosphate-buffered saline (PBS; pH 7.4) instead of the primary antibody; (2) treatment with PBS instead of the secondary antibody; and (3) the pre-adsorption of each antibody with its corresponding blocking molecules (Webster et al., 2021) (Supplementary Table S2). Sections of mammal tissues were used as positive controls and gave the expected results. Images of the IHC tests were obtained using a B-1000FL-HBO microscope (Optika, Bergamo, Italy) equipped with a digital camera (C-P20CC, 20 Mp, Optika) and image analysis software (Proview v.x64, Optika).

Double immunofluorescence

In the double-immunofluorescence protocols, primary antibody couples obtained from different host species (rabbit vs. mouse) were used to avoid cross-reaction due to immunoglobulin produced from the same host (rabbit vs. rabbit or mouse vs. mouse; see Table 1). Sections of the spiral intestine were dewaxed, re-hydrated, and rinsed in TBS with 0.05 % Triton-X100 (TBS-T) and then treated with 1:20 normal goat serum in TBS for 60 min in a humid chamber to inhibit non-specific reactions due to the secondary antibodies. The sections were incubated with the first primary antibody, generally, a rabbit polyclonal antibody (Supplementary Table S1), diluted in TBS for 24 h at room temperature (RT). The slides were then washed in TBS-T before the treatment with the avidin–biotin blocking solutions, as indicated in the manufacturer's guidelines (code SP-2001, Vector Lab., Burlingame, CA, USA). Thereafter, the sections were rinsed in TBS-T and incubated with 10 mg/mL of goat biotinylated anti-rabbit IgG (code BA-1000, Vector Lab.) in TBS for 3 h at RT. After a 2 × 5 min washing step in TBS-T, the sections were treated with 10 mg/mL of fluorescein–avidin D (code A-2001, Vector Lab.) in 0.1 M of $NaHCO_3$ (pH 8.5) with 0.15 M of NaCl for 3 h at RT. Afterward, the slides were incubated with the second primary antibody, generally, a mouse monoclonal antibody (Supplementary Table S1), diluted in TBS for 24 h at RT. The sections were rinsed twice for 5 min in TBS-T and then treated with 10 mg/mL of goat biotinylated anti-mouse IgG (code BA-9200, Vector Lab.) in TBS for 3 h at RT. After treatment, the slides were rinsed in TBS-T and then incubated with 10 mg/mL of rhodamine–avidin D (code A-2002, Vector Lab.) in 0.1 M of $NaHCO_3$ (pH 8.5) with 0.15 M of NaCl for 3 h at RT. The stained tissue sections were then mounted with the Vectashield® mounting medium with DAPI (code H-1002, Vector Lab.) and examined with an Olympus FV300 laser scanning confocal microscope (Olympus, Milan, Italy). All sections were excited using multi-argon/helio-neon green/UV lasers with excitation and barrier filters set for fluorescein, rhodamine, and DAPI. Green and red fluorescent signals from each antibody couple were obtained via alternate excitation (0.2 s^{-1}) at 488 nm and 540 nm, respectively, to avoid the cross-contamination of the two signals.

Evaluation of the co-localization of fluorescent signals

Four microscopic fields from three slides/specimens were selected for image acquisition in the double-immunofluorescence reactions. A 2 μm z-stack interval (18–21 optical sections) was set to obtain an image from each antibody couple, i.e., 12 images for channel N° 1 (detecting fluorescein) plus 12 images for channel N° 2 (detecting rhodamine) (4 microscopic fields × 3 slide/specimens). The image couples were opened in ImageJ 1.54f software and elaborated with the plugin JaCoP (Just Another Colocalization Plugin v.2.1.4, Bolte & Cordelières, 2006) to obtain Pearson's coefficient with Costes's automatic threshold. After discarding the lower and higher coefficient values from each double-immunofluorescence reaction, 10 Pearson's coefficient values were used to calculate the means ± standard error. The two antibody signals of a couple were considered co-localized with a mean Pearson's coefficient value of >0.500.

Results

The spiral intestine of the Blackmouth catshark is the longest intestinal region, placed between two short tracts, namely, the proximal and distal intestine. In the histological transversal section, the spiral intestine appeared as an internal spiral ring of epithelium with a connective axis forming epithelial folds, a lamina propria, and a thin smooth muscle layer whose thickness increased in the central region due to the high number of lympho-myeloid cells (Fig. 1a). The central region of the spiral intestine showed a connective framework of collagen fibers around smooth muscle cells and blood vessels (Fig. 1b). The Giemsa staining identified different cell types in the lympho-myeloid central

Table 1
Co-localization values for the double-immunofluorescence tests reported as means ± standard error of ten calculated measures of Costes's automatic threshold and Pearson's coefficient. The values were obtained from twenty confocal microscope-acquired z-stack images (ten from the green channel and ten from the red channel) for each antibody couple (see the text for an explanation). Only antibody couples obtained from different host species (MM-PR) were used. The bold values indicate the co-localization of the antibody couples.

Antibody anti-	Lysozyme (MM)	TLR-2 (PR)	Histamine (PR)	Serotonin (PR)	FCεRIγ (MM)	CD4 (PR)	IL-6 (MM)
Lysozyme (MM)							
TLR2 (PR)	**0.737 ± 0.027**						
Histamine (PR)	0.139 ± 0.040	—					
Serotonin (PR)	0.277 ± 0.047	—	—				
FCεRIγ (MM)	—	0.081 ± 0.019	**0.602 ± 0.017**	**0.876 ± 0.035**			
CD4 (PR)	**0.623 ± 0.032**	—	—	—	0.154 ± 0.033		
IL-6 (MM)	—	**0.580 ± 0.032**	0.155 ± 0.024	0.210 ± 0.021	—	0.150 ± 0.046	
TNF-α (PR)	**0.826 ± 0.042**	—	—	—	0.168 ± 0.035	—	**0.550 ± 0.061**

(MM): monoclonal mouse antibody; (PR): polyclonal rabbit antibody; CD4: cluster of differentiation 4; FCεRIγ: immunoglobulin E-like receptor; IL-6: interleukin-6; TLR2: toll-like receptor2; TNF-α: tumor necrosis factor-α.

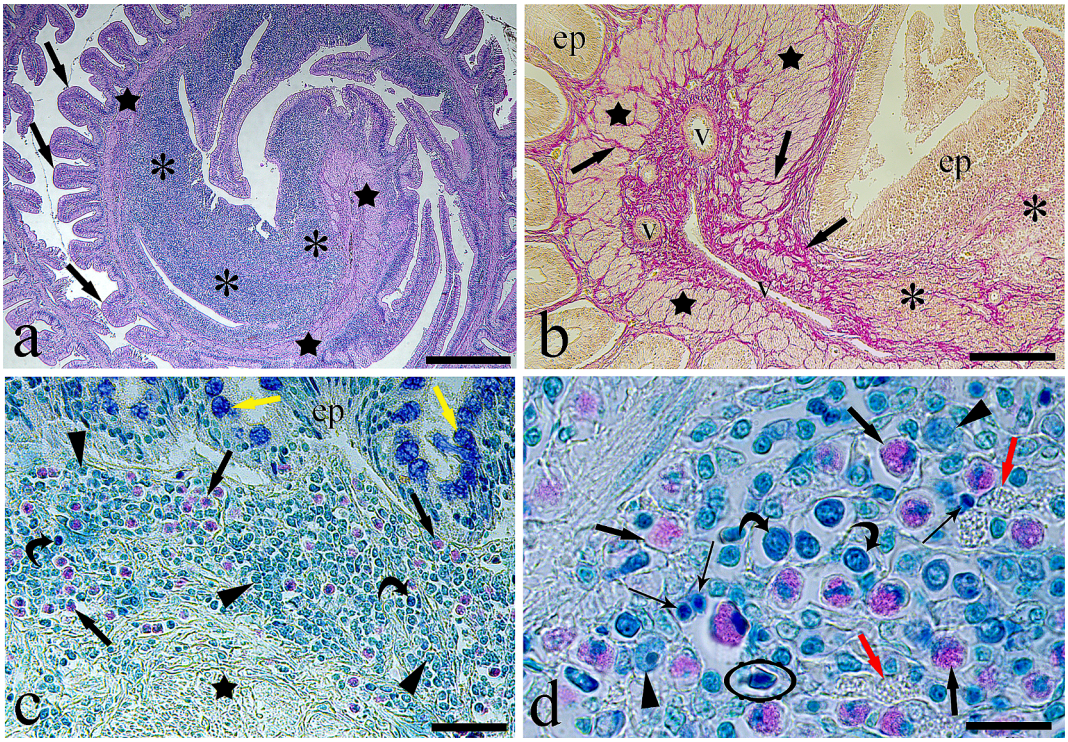

Fig. 1. Histology of the spiral intestine of *Galeus melastomus*. (a) Transverse section of the central spiral intestine. The mucosa rises in intestinal folds (arrows) with epithelium supported by a connective axis; the smooth muscle layer (stars) and a large lympho-myeloid cell aggregate (asterisks) thicken the spiral center. Hematoxylin and eosin—scale bar: 500 μm. (b) A dense collagen fiber network (arrows) supports the smooth muscle layer (stars) and the epithelium (ep) in the central spiral region, where blood vessels (v) are observed; asterisks indicate the lympho-myeloid cell aggregate. Sirius Red—scale bar: 200 μm. (c) The lympho-myeloid aggregate includes several immune cells, namely, eosinophilic cells (arrows), basophilic cells (arrowheads), and neutrophils (curved arrows). Stars and yellow arrows indicate the smooth muscle layer and mucous cells, respectively. ep: epithelium. Giemsa—scale bar: 50 μm. (d) High magnification of the lympho-myeloid cell aggregate with eosinophilic cells (arrows), basophilic cells (arrowheads), and neutrophils (curved arrows). Unstained cells (red arrows) with coarse cytoplasmic granulation, lymphocytes (thin arrows), and thrombocytes (ellipse) can also be observed. Giemsa—scale bar: 20 μm.

aggregate, namely, neutrophils, and basophilic and eosinophilic cells (Fig. 1c and d). Lymphocytes, thrombocytes, and unstained granulocytes with coarse cytoplasmic granules were noticed at a higher magnification (Fig. 1d).

In the lympho-myeloid aggregate of the spiral intestine, the anti-Toll-like receptor 2 (TLR2) antibody revealed two cell types, one bigger than the other (Fig. 2a). Moreover, intraepithelial cells positive to the anti-TLR2 antibody were documented (Fig. 2b). Immunoreactive cells with the anti-lysozyme antibody were located in the lympho-myeloid central aggregate (Fig. 2c), often near the blood vessels (Fig. 2d) and the intra-epithelial site (Fig. 2d). The same was observed for the anti-histamine antibody, where immuno-positive cells were encountered in the lympho-myeloid aggregate, the lamina propria, and the thickness of the epithelium (Fig. 3a and b). Several cells were immunoreactive with the anti-serotonin antibody in the lympho-myeloid aggregate and near the blood vessels (Fig. 3c and d). The anti-immunoglobulin E-like receptor (FCεRIγ) antibody revealed large cells of the lympho-myeloid aggregate (Fig. 3e). Intraepithelial cells that were immunoreactive with this antibody were also observed (Fig. 3f).

A high number of cells were immuno-positive to the anti-CD4 (Fig. 4a and b), -interleukin-6 (IL-6; Fig. 4c), and -TNF-α (Fig. 4d) antibodies in the lympho-myeloid aggregate of the spiral intestine. Cells positive to the anti-TNF-α antibody were seen in the epithelium near the basal membrane (Fig. 4e); this antibody was the only one that detected

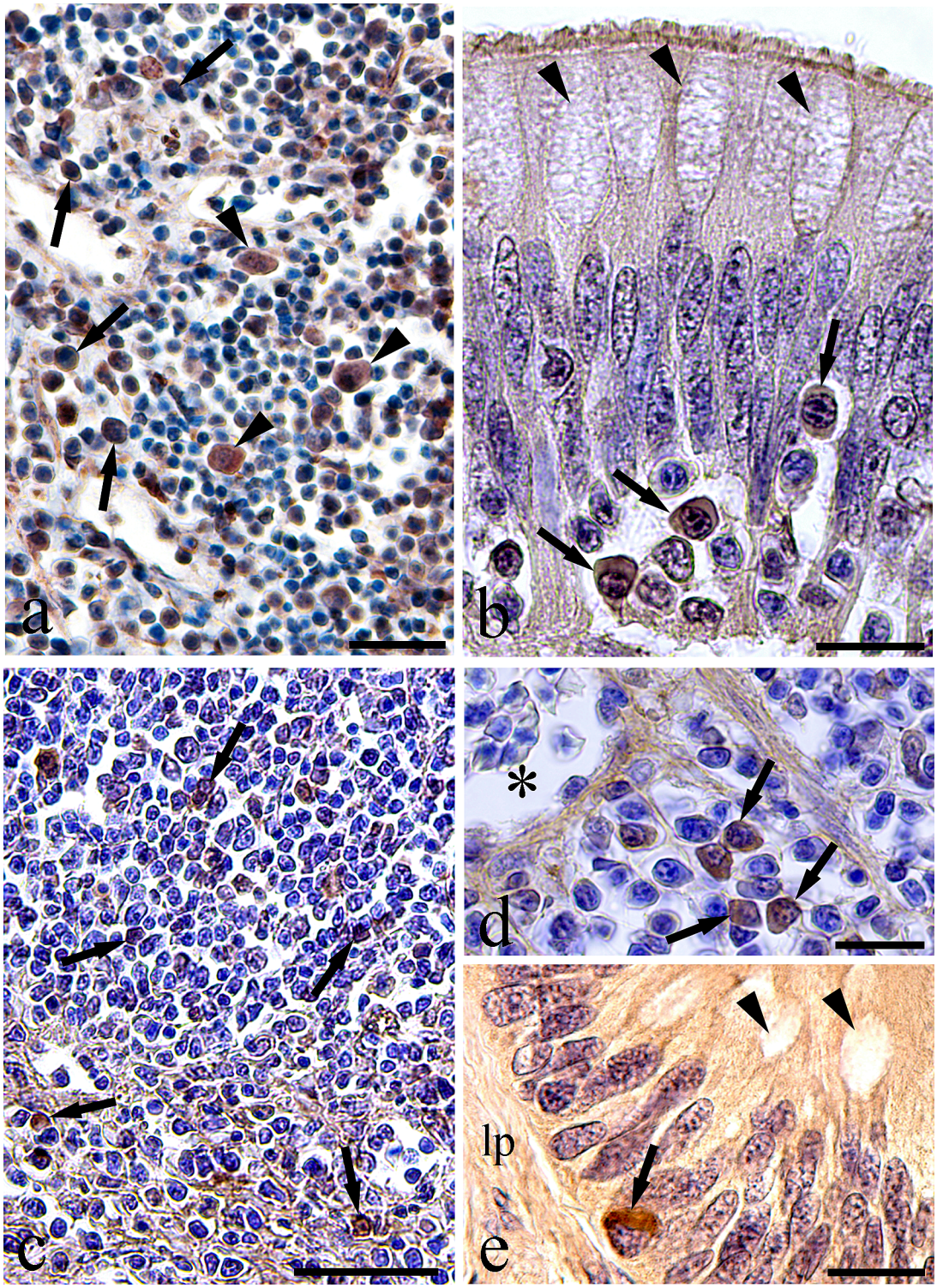

Fig. 2. Immunohistochemistry of the spiral intestine of *Galeus melastomus*. (a) In the lympho-myeloid aggregate, several cells (arrows) are immunoreactive with the anti-Toll-like receptor 2 (TLR2) antibody, among which large positive cells (arrowheads) are observed. Scale bar: 50 μm. (b) In the epithelium of the spiral intestine, anti-TLR2 immunoreactive cells (arrows) are detected; arrowheads indicate mucous cells. Scale bar: 20 μm. (c) Many cells (arrows) of the lympho-myeloid aggregate are immuno-positive to the anti-lysozyme antibody. Scale bar: 50 μm. (d) The high magnification shows anti-lysozyme immunoreactive cells (arrows) near a blood vessel (asterisk). Scale bar: 20 μm. (e). An intraepithelial cell (arrow) immunoreactive with the anti-lysozyme antibody on the basal membrane; arrowheads indicate mucous cells. Scale bar: 20 μm.

epithelial granular cells of the catshark spiral intestine (Fig. 4e; for comparison, see the unstained epithelial granular cells in Fig. 3f). The granulocytes with coarse cytoplasmic granules were not reactive with the eight used antibodies (Figs. 3e and 4b). Negative controls for the immunohistochemical procedures for all eight antibodies gave the expected results, as documented in Supplementary Fig. S1.

The JaCoP software (Bolte & Cordelières, 2006) elaboration of the double-immunofluorescence images showed cell co-localization for the

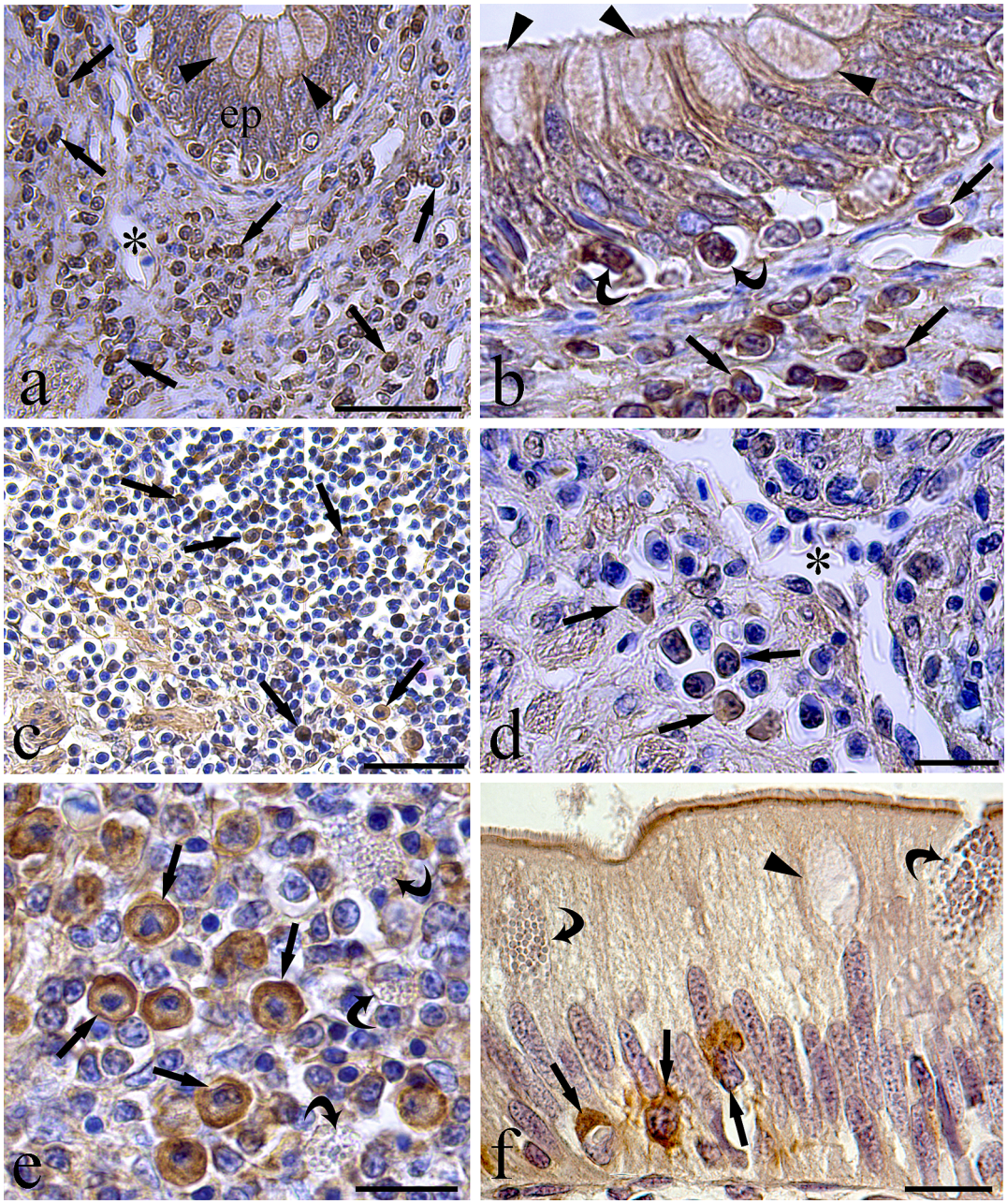

Fig. 3. Immunohistochemistry of the spiral intestine of *Galeus melastomus*. (a) The lympho-myeloid aggregate just below the epithelium (ep) presents several cells (arrows) immunoreactive with the anti-histamine antibody. The asterisks and arrowheads indicate a blood vessel and mucous cells, respectively. Scale bar: 50 μm. (b) The high magnification shows anti-histamine immuno-positive cells within the epithelium (curved arrows) and in the underlying connective tissue (arrows). Mucous cells are indicated by arrowheads. Scale bar: 20 μm. (c) A large number of cells (arrows) immunoreactive with the anti-serotonin antibody is observed in the lympho-myeloid aggregate. Scale bar: 100 μm. (d) The high magnification shows anti-serotonin immunoreactive cells (arrows) near a blood vessel (asterisk). Scale bar: 50 μm. (e) Large-size cells (arrows) are detected by the anti-immunoglobulin E-like receptor (FCεRIγ) antibody in the lympho-myeloid aggregate. Note the unstained cells (curved arrows) with coarse cytoplasmic granules. Scale bar: 20 μm. (f). In the intestinal epithelium, anti-FCεRIγ immunoreactive cells (arrows) are observed near the basal membrane. The curved arrows and the arrowhead show two unstained epithelial granular cells and a mucous cell, respectively. Scale bar: 20 μm.

anti-lysozyme antibody with the anti-TLR2, -CD4, and -TNF-α antibodies (Fig. 5a–c and Table 1). Moreover, lympho-myeloid cells co-localized the anti-IL-6 antibody with the anti-TLR2 and -TNF-α antibodies (Table 1). The anti-FCεRIγ antibody showed cell co-localization with the anti-histamine and -serotonin antibodies (Fig. 5d and e, Table 1, respectively). Three examples of non-co-localization of the immune markers are reported in Fig. 6, namely, the anti-histamine and -lysozyme and anti-FCεRIγ antibodies with the anti-TNF-α and -TLR2 antibodies (Fig. 6a–c and Table 1, respectively).

Discussion

The elasmobranchs are the most primitive vertebrates to exhibit an immune response and have true lymphoid organs, such as the thymus, spleen, and GALT (Zapata et al., 1996). The GALT consists of individual immune cells in the epithelium and lamina propria, as well as leukocyte accumulation in the lamina propria (Hart et al., 1987; Lauriano et al., 2019). In the spiral intestine of *G. melastomus*, the GALT was primarily composed of a non-encapsulated central aggregate of lympho-myeloid cells. In mammals, the GALT is a secondary immune tissue mainly

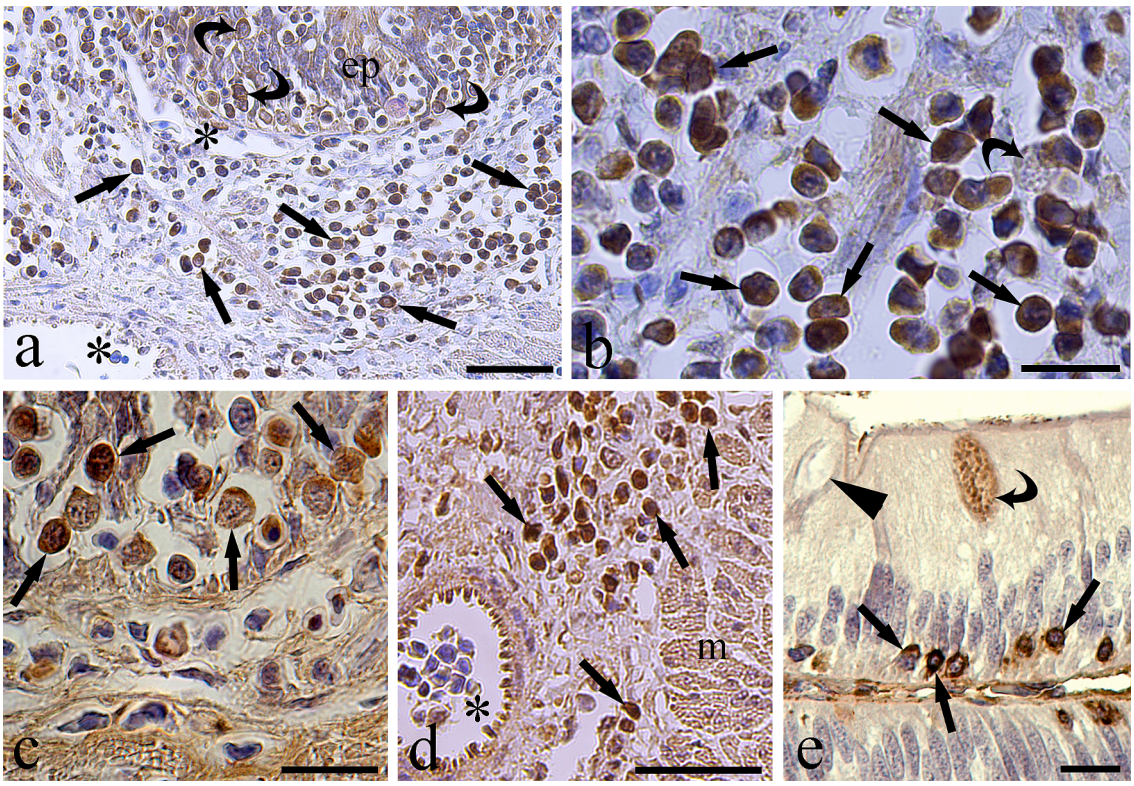

Fig. 4. Immunohistochemistry of the spiral intestine of *Galeus melastomus*. (a) In the lympho-myeloid aggregate, several cells (arrows) just below the epithelium (ep) and cells (curved arrows) in the thickness of the epithelium are immunoreactive with the anti-CD4 antibody. Asterisks indicate blood vessels. Scale bar: 50 μm. (b) The high magnification shows the anti-CD4 immuno-positive cells (arrows) in the lympho-myeloid aggregate; note the unstained cell (curved arrow) with coarse cytoplasmic granules. Scale bar: 20 μm. (c). Cells (arrows) immunoreactive with the anti-interleukin-6 (IL-6) antibody are observed in the lympho-myeloid aggregate. Scale bar: 20 μm. (d) The image shows diverse cells (arrows) immunoreactive with the anti-tumor necrosis factor-α (TNF-α) antibody in the lympho-myeloid aggregate near a blood vessel (asterisk). m: smooth muscle layer. Scale bar: 50 μm. (e) Many cells (arrows) close to the basal membrane of the epithelium are immunoreactive with the anti-TNF-α antibody. The curved arrow and the arrowhead show an anti-TNF-α immunoreactive granular epithelial cell and a mucous cell, respectively. Scale bar: 20 μm.

serving the intestinal mucosa and is composed of encapsulated lymphoid aggregates called Peyer's patches (Mitchell & Criscitiello, 2020). Elasmobranchs lack Peyer's patches, but they have non-encapsulated lymphoid aggregates in the spiral intestine (Mitchell & Criscitiello, 2020; Smith et al., 2019). Although the GALT in the spiral intestine is not considered a true lymphoid organ, it was proposed as a primitive ancestor of Peyer's patches (Boehm et al., 2012).

Insight into the morphology of the spiral intestine in *G. melastomus* was presented in Bosi et al. (2022), and the current study provides further details. The spiral intestine has many similarities to that of other cartilaginous fish described in (Chatchavalvanich et al., 2006; Lauriano et al., 2019; Sayyaf Dezfuli et al., 2018a, 2019). The spiral intestine of the Blackmouth catshark showed an internal fold consisting of the epithelium, lamina propria, and lamina muscularis wrapped in a spiral with a thickened central region containing the GALT. The central region of the spiral intestine contains a high concentration of leukocytes (Zapata et al., 1996).

Several accounts dealt with the histological and ultrastructural aspects of the GALT cells of elasmobranchs showing the presence of lymphocytes, plasma cells, macrophages, and granulocytes with different cytoplasmic granules (Hart et al., 1987; Zapata et al., 1996). In most elasmobranchs, granulocytes are classified into three types based on the cell ultrastructure and staining properties of their cytoplasmic granules: (a) the most common heterophils or fine eosinophilic granulocytes, named G1 granulocytes; (b) G2 granulocytes similar to mammalian neutrophils; and (c) G3 coarse eosinophilic granulocytes (Smith et al., 2019). Herein, the following cells were recognized in the GALT of *G. melastomus* via Giemsa staining: G1 granulocytes, G2 granulocytes, unstained G3 granulocytes, basophils, lymphocytes, and thrombocytes. Basophils were reported in the blood of *Neoceratodus forsteri*, the Australian lungfish, and in many other shark species (Hine, 1992). Basophils are rare in the elasmobranchs and are classified as non-eosinophilic granulocytes (Carmezim & Marcos, 2020). Basophils were observed in the epigonal and Leydig's organs of *Rhizoprionodon lalandii*, the Brazilian sharpnose shark. It was suggested that basophils are the immature stage of G1 granulocytes (Pacheco et al., 2002); likewise, basophils in the GALT of *G. melastomus* can be considered as immature cells of the granulocytes lineage.

The exact immune cell identification in elasmobranchs remains open to conjecture because of species-specific patterns and different tinctorial properties due to the histological staining and the presence of immature cells in the peripheral blood (Carmezim & Marcos, 2020; Hine & Wain, 1987). Enzyme cytochemistry has been employed to distinguish and differentiate between the peripheral granulocytes in several species of elasmobranchs (see Hine & Wain, 1987). Hine and Wain were among the first to distinguish between shark granulocytes (Hine & Wain, 1987) in the blood of 13 species of sharks and 4 species of skates using enzyme cytochemistry. However, the authors found similarities in the acidic hydrolases of the blood granulocytes in these species, indicating the general phagocytic function of different granulocyte types (Hine & Wain, 1987). Lymphocytes and granulocytes in the spiral intestine of *N. forsteri* were analyzed using flow cytometry assays on their viability, phagocytotic activity, oxidative burst, and apoptosis (Hassanpour et al., 2013). Recently, the GALT of sharks and rays was investigated with immunohistochemical approaches (Lauriano et al., 2019; Sayyaf Dezfuli et al., 2018a, 2019).

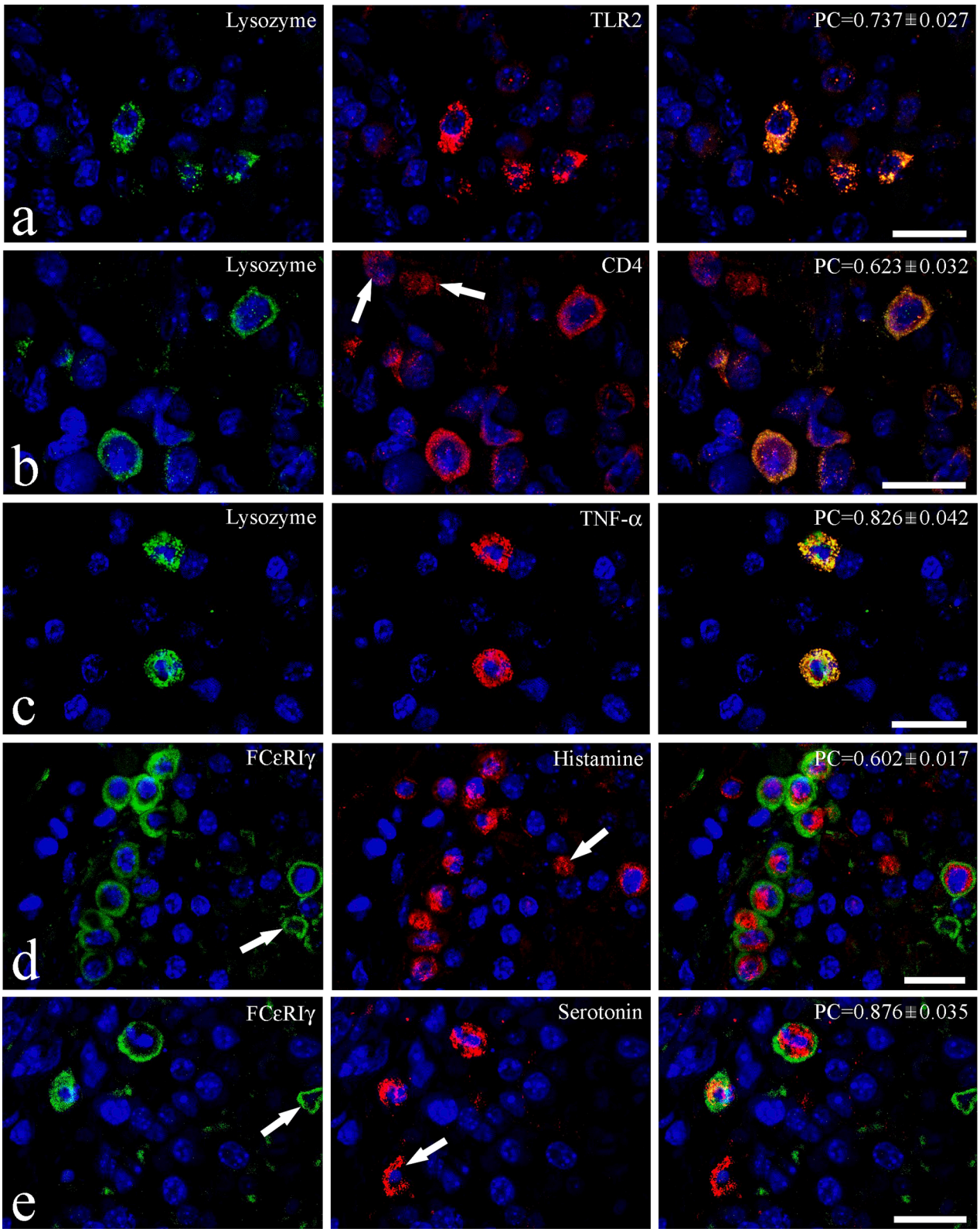

Fig. 5. Double-immunofluorescence of the lympho-myeloid aggregate in the spiral intestine of *Galeus melastomus*. Each line shows the fluororeactive cells with the FITC-bound antibody (first column) and the Rhodamine-bound antibody (second column) of a couple used in the double immunofluorescence procedure. The antibody type is reported in each image. The third column of each line shows the merged image obtained via the superimposition of the first- and second-column images; the mean values (±standard error) of Pearson's coefficient with Costes's automatic threshold are reported at the top right (see explanation in Materials and Methods). Values of >0.500 show a positive co-localization of the two detected immune antibody markers. (a), (b), (c), (d), and (e)—scale bars: 20 μm. (b) In the second-column image, the arrows indicate two immunofluororeactive cells with only the anti-CD4 antibody. (d) In the first- and second-column images, the arrows show a cell fluororeactive only with the anti-FCεRIγ antibody and only with the anti-histamine antibody, respectively. (e) In the first- and second-column images, the arrows show a cell fluororeactive only with the anti-FCεRIγ antibody and only with the anti-serotonin antibody, respectively.

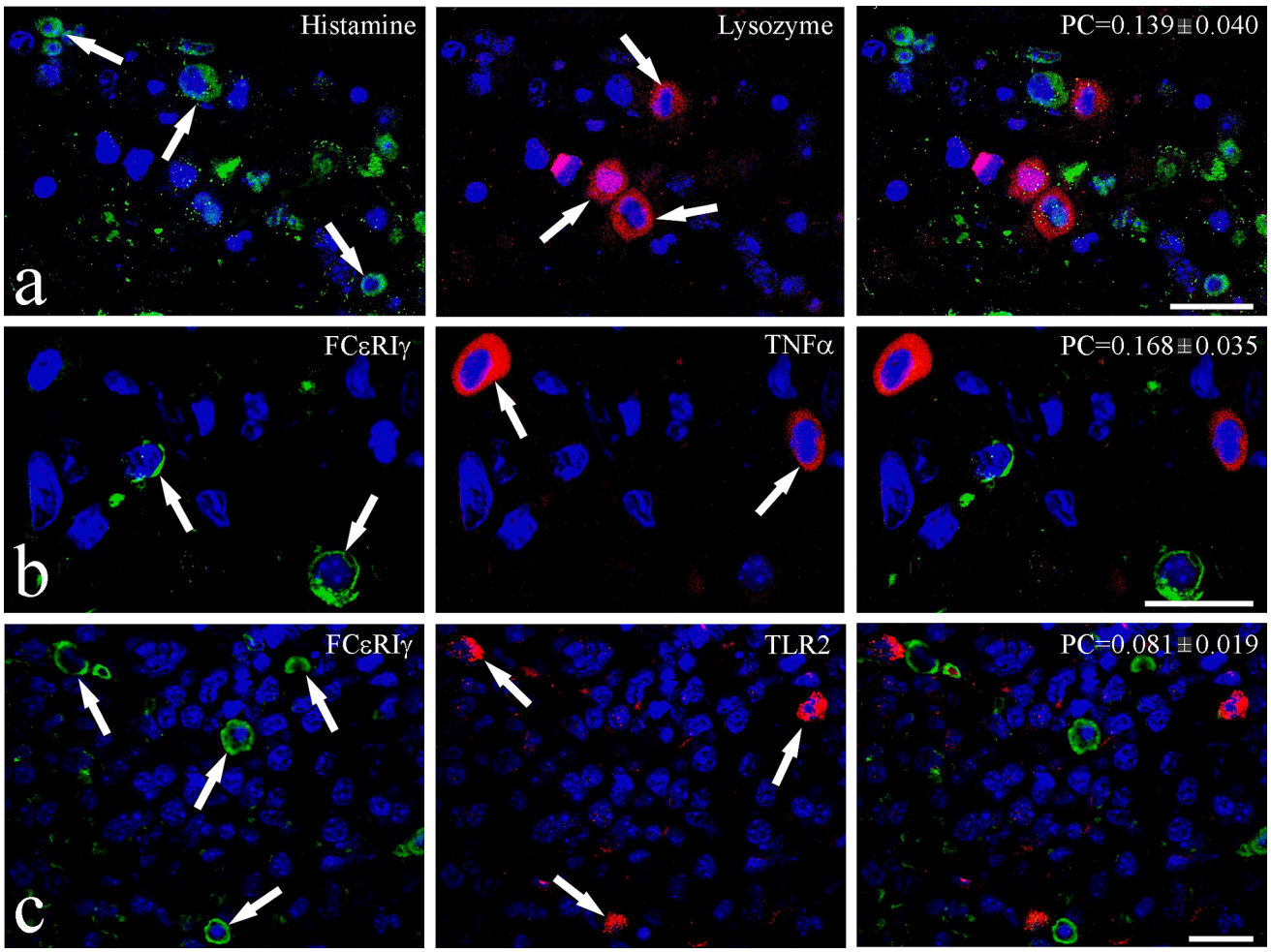

Fig. 6. Double-immunofluorescence of the lympho-myeloid aggregate in the spiral intestine of *Galeus melastomus*. Each line shows the fluororeactive cells for the FITC-bound antibody (first column) and the Rhodamine-bound antibody (second column) of a couple used in the double-immunofluorescence procedure; the antibody type is reported in each image. The third column of each line shows the merged image obtained via the superimposition of the first- and second-column images; the mean values (±standard error) of Pearson's coefficient with Costes's automatic threshold are reported at the top right (see explanation in Materials and Methods). Values of <0.500 show no co-localization of the two detected immune antibody markers. (a) In the first- and second-column images, the arrows show cells fluororeactive only with the anti-histamine antibody and only with the anti-lysozyme antibody, respectively. (b) In the first- and second-column images, the arrows show cells fluororeactive only with the anti-FCεRIγ antibody and only with the anti-TNF-α antibody, respectively. (c) In the first- and second-column images, the arrows show cells fluororeactive only with the anti-FCεRIγ antibody and only with the anti-TLR2 antibody, respectively. Scale bars: 20 μm.

Several cells immunopositive to the anti-histamine and -serotonin antibodies were observed in the spiral intestine of the Blackmouth catshark, often located near blood vessels or the basal membrane of the epithelium. The above two biogenic amines are secreted and stored in fish mast cells and are involved in the inflammatory process due to gut infection by parasites (Sayyaf Dezfuli et al., 2018b, 2021, 2023a, 2023b). The first absolute record of the presence of histamine in the mast cells of a fish, *Sparus aurata*, a member of the order Perciformes, the most evolutionarily advanced teleosts, appeared in Mulero et al. (2007). Evidence of mast cells containing histamine and serotonin in a Perciformes fish that harbored an enteric helminth was provided in Sayyaf Dezfuli et al. (2018b). The authors stressed that histamine and serotonin have been highly conserved as biogenic amines throughout the fish's evolution (El-Salhy et al., 1985; Reite, 1972, respectively). Herein, the presence of these molecules was documented in the granulocytes in the spiral intestine of *G. melastomus*; thus, our findings reinforce the concept of histamine and serotonin being highly conserved during evolution.

In mammals, the chemical bond between the immunoglobulin E (IgE)-like receptor (FCεRIγ) and the antigen–IgE complex on the plasmalemma of mast cells induces the release of histamine and serotonin (Kraft & Kinet, 2007). The FCεRIγ-like receptor was observed in the mast cells of different fish species in (Da'as et al., 2011; Sayyaf Dezfuli, 2018b). In the GALT of *G. melastomus*, the anti-FCεRIγ antibody was noticed in big-size cells resembling immunoreactive cells with anti-histamine and -serotonin. Moreover, anti-FCεRIγ-positive cells were observed in the intra-epithelial site. The presence of an FCεRIγ-like receptor in the intestinal granulocytes of the catshark provides further evidence of FCεRIγ's involvement in the amine release and activation of the immune-specific response, as substantiated in Da'as et al. (2011) and Sayyaf Dezfuli et al. (2018b).

Toll-like receptors (TLRs) belong to pattern recognition receptors (PRRs) and reveal molecules of pathogenic origin (i.e., pathogen-associated molecular patterns (PAMPs)) or molecules released by damaged cells (i.e., damage-associated molecular patterns (DAMPs)) (Alesci & Lauriano et al., 2020; Sudhagar et al., 2020). Many types of TLRs have been identified and sequenced in different vertebrate taxa, with 28 TLR types existing only in fish (Dalmo & Bøgwald, 2022). Interestingly, their structures and genotypes are highly conserved in vertebrates (Anandhakumar et al., 2012). Among the TLRs, TLR2 is involved in the detection of lipopolysaccharides and peptidoglycan in the innate immune response (Zhang et al., 2014). TLR2 leads to the activation of macrophages via the production of cytokines and

chemokines and the amplification of the immune response (Alesci & Lauriano et al., 2020; Korenaga et al., 2013).

Data on the presence and expression level of the cytoplasmic signaling domain for the TLR2 in a lip shark *Chiloscyllium* sp. were first reported in Anandhakumar et al. (2012). Moreover, the authors documented the highest expression level for TLR2-TIR mRNA in the following immune organs: the kidneys, spleen, epigonal organ, and spiral intestine. TLR2 was mainly localized in macrophages and lymphoid cells (Anandhakumar et al., 2012). A phylogenetic analysis revealed over 75 % of nucleotide identity for TLR2 in lip sharks, teleosts, and mammals (Anandhakumar et al., 2012). The anti-TLR2 antibody in the GALT of *G. melastomus* was encountered in large cells, closely resembling macrophages, and in dendritic cells, as previously noted in the GALT of another shark *S. canicula* in Lauriano et al. (2019). Anti-TLR2 marked the intraepithelial lymphocytes in the spiral intestine of *S. canicula* (Lauriano et al., 2019), and a similar finding was observed in *G. melastomus* in this study.

CD4 is a transmembrane peptide with four extracellular immunoglobulin-like domains and a cytoplasmic tail responsible for intracellular signaling (Smith et al., 2019). T helper cells, monocytes/macrophages, and dendritic cells have CD4 (Schridde et al., 2017; Smith et al., 2019). The chemical bond between CD4 and antigens formed via major histocompatibility complex II (MHC II) stimulates the release of cytokines by T helper cells (Alberts et al., 2002). Herein, several immunoreactive cells with the anti-CD4 antibody were observed in the lympho-myeloid aggregate of the Blackmouth catshark spiral intestine. Based on their size and CD4 being identified as a molecular marker expressed in most mature macrophages (Schridde et al., 2017; Shaw et al., 2018), it would be reasonable to suppose these cells are macrophages. However, there is insufficient information on the biological functions of CD4 in elasmobranchs, and more studies are needed, as pointed out in (Smith et al., 2019).

One of the most studied components in the innate immune system of fish is lysozyme (Smith et al., 2019), a lytic enzyme whose main defensive activity is the disruption of the bacterial wall, resulting in the lysis of the pathogen (Myrnes et al., 2013). Moreover, its selected effects involve the activation of the complement system, opsonization, and phagocytosis (Smith et al., 2019). Immunoreactivity against the anti-lysozyme antibody was observed in GALT and intraepithelial cells in the *G. melastomus* spiral intestine. The occurrence of lysozyme in the lympho-myeloid tissue in four elasmobranch species and one marine teleost was first reported in Lundblad et al. (1979).

Lysozyme was characterized and its ability to hydrolyze and inhibit the growth of bacteria was demonstrated in a molecular investigation on the nurse shark *Ginglymostoma cirratum* (Hinds Vaughan & Smith, 2013). Anti-lysozyme immunoreactive elements were observed in “type I granular cells” within the intestinal epithelium of the ray *Raja clavata* (Sayyaf Dezfuli et al., 2018a). It is generally agreed that lysozyme is involved in the first line of defense against pathogens, and its functions are similar in cartilaginous and bony fish (Hinds Vaughan & Smith, 2013; Lundblad et al., 1979; Sayyaf Dezfuli et al., 2018a; Smith et al., 2019).

The cytokine IL-6 is a pro-inflammatory peptide that is quickly and transiently secreted against the presence of viruses and bacteria or after the release of other signaling molecules (Sayyaf Dezfuli et al., 2018a; Zou & Secombes, 2016). IL-6 was found in neutrophils and macrophages of most fish species (Korenaga et al., 2013; Pérez-Cordón et al., 2014; Sayyaf Dezfuli et al., 2018a; Zou & Secombes, 2016). Its release from activated macrophages is induced by the chemical bond between TLR and a PAMP molecule (Korenaga et al., 2013). Increased secretion of IL-6 was reported in the intestine of *S. aurata* infected with the myxozoan *Enteromyxum leei* (Pérez-Cordón et al., 2014). Furthermore, a high number of immune cells expressed IL-6 in the intestine of the pike *Esox lucius* infected with the acanthocephalan *Acanthocephalus lucii* (Sayyaf Dezfuli et al., 2018b). In the GALT of *G. melastomus*, several immune cells were immunoreactive with the anti-IL-6 antibody; similarly, the “type III intestinal granular cells” of the ray *R. clavata* also showed a positive reaction with the same antibody (Sayyaf Dezfuli et al., 2018a). IL-6 has a mediatory role between the innate and adaptive immune responses during inflammation (Naka et al., 2002; Sayyaf Dezfuli et al., 2018a). The spiral intestine of elasmobranchs slows the transit of digesta in favor of an increase in nutrient uptake (Bosi et al., 2022); however, containing a large amount of food might increase the bacterial charge, including harmful species. In all vertebrates, the alimentary canal represents one of the main entry points for pathogen invasion of the host body; thus, the expression of IL-6 by the immune cells of the catshark spiral intestine is reasonable.

In addition to the secretion of IL-6, the activation of macrophages in fish produces TNF-α, a pro-inflammatory cytokine with a variety of physiological functions (Pérez-Cordón et al., 2014; Smith et al., 2019). TNF-α is secreted by cell types such as epithelial cells and mast cells (Sayyaf Dezfuli et al., 2018a, 2018b). The secretion of TNF-α is related to cell proliferation, the modulation of immune cells, and the regulation of cytokine production (Seno et al., 2002). Immune cell aggregates, especially near blood vessels, as well as immunoreactive intraepithelial cells with the anti-TNF-α antibody, were documented in the spiral intestine of the Blackmouth catshark. The “type I granular cell” of *R. clavata* was often located near the basal membrane and was immunoreactive with the same antibody (Sayyaf Dezfuli et al., 2018a). We documented the occurrence of anti-TNF-α immunoreactive granular cells at the epithelial apex in the intestinal epithelium of *G. melastomus* (see Fig. 4e). The granules of these cells were strongly eosinophilic and immunoreactive with the anti-TNF-α antibody (Sayyaf Dezfuli et al., 2019). Similarly, epithelial cells with eosinophilic granules were suggested to function like mammalian Paneth cells in the spiral intestine of *Polyodon spathula*, the American paddlefish (Petrie-Hanson & Peterman, 2005). Paneth cells secrete defensive molecules such as lysozyme and TNF-α (Seno et al., 2002). Although the granular epithelial cells in the Blackmouth catshark were not immunoreactive with the anti-lysozyme antibody, it was postulated that they might act as Paneth cells (Sayyaf Dezfuli et al., 2019).

In this study, a confocal microscope detected the co-expression of molecular immune markers in the cells of the *G. melastomus* GALT. We used antibody-searching molecules for mast cells (i.e., histamine, serotonin, and FCeRIg) and the monocyte/macrophage lineage (i.e., TLR2, lysozyme, CD4, IL-6, and TNF-α) tested in several fish species by other authors (Hine, 1992; Myrnes et al., 2013; Pacheco et al., 2002; Sayyaf Dezfuli et al., 2023b).

Dendritic cells co-expressed TLR2/langerin and TLR2/MHC II in the intestinal lamina propria of the small-spotted catfish (Alesci & Capillo et al., 2022). Cells resembling macrophages co-expressed TLR2/lysozyme and TLR2/IL-6 in the GALT of *G. melastomus*. Macrophages and dendritic cells act as antigen-presenting cells (APCs), which are essential to activate the immune response by T lymphocytes (Alesci & Capillo et al., 2022). The APCs are able to recognize a wide variety of pathogens molecules, the so-called “pathogen associated molecular patterns” (Sudhagar et al., 2020) and bind these antigens to the Major Histocompatibility Complex proteins on their cell surface. Lymhocytes T are activated after the recognition of this complex formed by APCs (Smith et al., 2019).

Granulocytes related to the macrophage lineage co-express cytokines (TNF-α/IL-6) and lysozyme with TNF-α and CD4. IL-6 and CD4 are also expressed by activated T lymphocytes (Shaw et al., 2018; Zou & Secombes, 2016). The co-presence of IL-6 with TNF-α and CD4 with lysozyme indicates that the immunofluororeactive cells in the Blackmouth catshark GALT were macrophages. In the lysozyme/CD4 double-immunofluorescence test, some small-size immune cells appeared positive only for the anti-CD4 antibody (see Fig. 5b) and could be T lymphocytes. In the GALT of *G. melastomus*, histamine and FCεRIγ, as well as serotonin and FCεRIγ, were co-expressed in a granulocyte lineage and are most likely mast cells.

Conclusions

The GALT of *G. melastomus* contains a lympho-myeloid cell aggregate, with dominating macrophages and two types of granulocytes, fine cytoplasmic granulocytes, and neutrophils. The coarse cytoplasmic granulocytes were scarce and unreactive with the different staining and eight antibodies tested. The immunohistochemical and double immunofluorescence protocols revealed the presence of a mast cell-like lineage co-expressing histamine/FCεRIγ and serotonin/FCεRIγ. A macrophage lineage with reactivity and co-presence for lysozyme, CD4, TNF-α, TLR2, and IL-6 was noticed. We reported the co-expression results for this panel of markers in the GALT of an elasmobranch for the first time. The occurrence of immune cells containing specific defensive molecules confirms that the spiral intestine alimentary canal is a vulnerable site for action of the pathogens that needs an efficient immune system. In elasmobranchs, further researches are in progress on the immune cells of granulopoietic tissues like Leydig's and the epigonal organs. Cartilaginous fish are key in the evolution of vertebrates and surprisingly exhibit several features of the mammalian protection system; thus, studying shark defensive cells is essential to improve the understanding of higher vertebrate immunity.

CRediT authorship contribution statement

Giampaolo Bosi: Writing – original draft, Validation, Methodology, Formal analysis, Conceptualization. **Bahram Sayyaf Dezfuli:** Writing – review & editing, Validation, Resources, Funding acquisition, Data curation, Conceptualization. **Paolo Merella:** Writing – review & editing, Resources, Methodology. **Luisa Giari:** Writing – review & editing, Validation, Methodology, Formal analysis, Data curation, Conceptualization.

Declaration of competing interest

The authors declare that they have no known competing financial interests or personal relationships that could have appeared to influence the work reported in this paper.

Acknowledgements

Special thanks to the staff of the fishing boat Firm Rum belonging to Antonio & Umberto S.N.C. for providing the samples. This work was supported by local grants from the University of Ferrara to B. Sayyaf Dezfuli and Luisa Giari (grant number FAR 2023).

Ethical clearance statement

Not applicable.

Appendix A. Supplementary data

Supplementary data to this article can be found online at https://doi.org/10.1016/j.ejar.2024.10.002.

References

Alberts, B., Johnson, A., Lewis, J., Raff, M., Roberts, K., & Walter, P. (2002). *Molecular biology of the cell* (4th ed.). Garland Science.

Alesci, A., Capillo, G., Fumia, A., Messina, E., Albano, M., Aragona, M., Lo Cascio, P., Spanò, N., Pergolizzi, S., & Lauriano, E. R. (2022). Confocal characterization of intestinal dendritic cells from Myxines to Teleosts. *Biology, 11*(7), 1045. https://doi.org/10.3390/biology11071045

Alesci, A., Lauriano, E. R., Aragona, M., Capillo, G., & Pergolizzi, S. (2020). Marking vertebrates langerhans cells, from fish to mammals. *Acta Histochemica, 122*(7), Article 151622. https://doi.org/10.1016/j.acthis.2020.151622

Anandhakumar, C., Lavanya, V., Pradheepa, G., Tirumurugaan, K. G., Dhinakar Raj, G., Raja, A., Pazhanivel, N., & Balachandran, C. (2012). Expression profile of toll-like receptor 2 mRNA in selected tissues of shark (*Chiloscyllium sp.*). *Fish & Shellfish Immunology, 33*(5), 1174–1182. https://doi.org/10.1016/j.fsi.2012.09.007

Boehm, T., Hess, I., & Swann, J. B. (2012). Evolution of lymphoid tissues. *Trends in Immunology, 33*(6), 315–321. https://doi.org/10.1016/j.it.2012.02.005

Bolte, S., & Cordelières, F. P. (2006). A guided tour into subcellular colocalization analysis in light microscopy. *Journal of Microscopy, 224*(3), 213–232. https://doi.org/10.1111/j.1365-2818.2006.01706.x

Bosi, G., Merella, P., Maynard, B. J., & Sayyaf Dezfuli, B. (2022). Microscopic characterization of the mucous cells and their mucin secretions in the alimentary canal of the Blackmouth catshark *Galeus melastomus* (Chondrichthyes: Elasmobranchii). *Fishes, 7*(1), 8. https://doi.org/10.3390/fishes7010008

Bosi, G., Shinn, A. P., Giari, L., & Sayyaf Dezfuli, B. (2015). Enteric neuromodulators and mucus discharge in a fish infected with the intestinal helminth *Pomphorhynchus laevis*. *Parasites & Vectors, 8*, 359. https://doi.org/10.1186/s13071-015-0970-7

Carmezim, H. S., & Marcos, R. (2020). There is plenty more fish nomenclature in the sea: The elasmobranch granulocytes. *Veterinary Clinical Pathology, 49*(2), 196–197. https://doi.org/10.1111/vcp.12875

Chatchavalvanich, K., Marcos, R., Poonpirom, J., Thongpan, A., & Rocha, E. (2006). Histology of the digestive tract of the freshwater stingray *Himantura signifer* Compagno and Roberts, 1982 (Elasmobranchii, Dasyatidae). *Anatomy and Embryology, 211*, 507–518. https://doi.org/10.1007/s00429-006-0103-3

Da'as, S., Teh, E. M., Dobson, J. T., Nasrallah, G. K., McBride, E. R., Wang, H., Neuberg, D. S., Marshall, J. S., Lin, T.-J., & Berman, J. N. (2011). Zebrafish mast cells possess an FcεRI-like receptor and participate in innate and adaptive immune responses. *Developmental and Comparative Immunology, 35*(1), 125–134. https://doi.org/10.1016/j.dci.2010.09.001

Dalmo, R. A., & Bøgwald, J. (2022). Innate Immunity. In K. Buchmann, & C. J. Secombes (Eds.), *Principles of fish immunology: From cells and molecules to host protection* (pp. 31–103). Springer International Publishing. https://doi.org/10.1007/978-3-030-85420-1_2.

El-Salhy, M., Wilander, E., & Lundqvist, M. (1985). Comparative studies of serotonin-like immunoreactive cells in the digestive tract of vertebrates. *Biomedical Research, 6*(6), 371–375. https://doi.org/10.2220/biomedres.6.371

Farrag, M. M. (2016). Deep-sea ichthyofauna from Eastern Mediterranean Sea, Egypt: Update and new records. *The Egyptian Journal of Aquatic Research, 42*(4), 479–489. https://doi.org/10.1016/j.ejar.2016.12.005

Hart, S., Wrathmell, A. B., Harris, J. E., & Doggett, T. A. (1987). Gut-associated lymphoid tissue (GALT) in the common dogfish *Scyliorhinus canicula* L.: An ultrastructural study. *Journal of the Marine Biological Association of the United Kingdom, 67*(3), 639–645. https://doi.org/10.1017/S002531540002734X

Hassanpour, M., Joss, J., & Mohammad, M. G. (2013). Functional analyses of lymphocytes and granulocytes isolated from the thymus, spiral valve intestine, spleen, and kidney of juvenile Australian lungfish, *Neoceratodus Forsteri*. *Fish & Shellfish Immunology, 35*(1), 107–114. https://doi.org/10.1016/j.fsi.2013.04.006

Hinds Vaughan, N., & Smith, S. L. (2013). Isolation and characterization of a c-type lysozyme from the nurse shark. *Fish & Shellfish Immunology, 35*(6), 1824–1828. https://doi.org/10.1016/j.fsi.2013.09.001

Hine, P. M. (1992). The granulocytes of fish. *Fish & Shellfish Immunology, 2*(2), 79–98. https://doi.org/10.1016/S1050-4648(05)80038-5

Hine, P. M., & Wain, J. M. (1987). The enzyme cytochemistry and composition of elasmobranch granulocytes. *Journal of Fish Biology, 30*(4), 465–475. https://doi.org/10.1111/j.1095-8649.1987.tb05770.x

Korenaga, H., Nagamine, R., Sakai, M., & Kono, T. (2013). Expression profile of cytokine genes in Fugu monocytes stimulated with TLR agonists. *International Immunopharmacology, 17*(2), 390–399. https://doi.org/10.1016/j.intimp.2013.07.004

Kraft, S., & Kinet, J.-P. (2007). New developments in FcεRI regulation, function and inhibition. *Nature Reviews Immunology, 7*(5), 365–378. https://doi.org/10.1038/nri2072

Lauriano, E. R., Pergolizzi, S., Aragona, M., Montalbano, G., Guerrera, M. C., Crupi, R., Faggio, C., & Capillo, G. (2019). Intestinal immunity of dogfish *Scyliorhinus canicula* spiral valve: A histochemical, immunohistochemical and confocal study. *Fish & Shellfish Immunology, 87*, 490–498. https://doi.org/10.1016/j.fsi.2019.01.049

Lundblad, G., Fänge, R., Slettengren, K., & Lind, J. (1979). Lysozyme, chitinase and exo-N-acetyl-β-D-glucosaminidase (NAGase) in lymphomyeloid tissue of marine fishes. *Marine Biology, 53*, 311–315. https://doi.org/10.1007/BF00391613

Mitchell, C. D., & Criscitiello, M. F. (2020). Comparative study of cartilaginous fish divulges insights into the early evolution of primary, secondary and mucosal lymphoid tissue architecture. *Fish & Shellfish Immunology, 107*, 435–443. https://doi.org/10.1016/j.fsi.2020.11.006

Mulero, I., Sepulcre, M. P., Meseguer, J., García-Ayala, A., & Mulero, V. (2007). Histamine is stored in mast cells of most evolutionarily advanced fish and regulates the fish inflammatory response. *Proceedings of the National Academy of Sciences of the United States of America, 104*(9), 19434–19439. https://doi.org/10.1073/pnas.0704535104

Myrnes, B., Seppola, M., Johansen, A., Øverbø, K., Callewaert, L., Vanderkelen, L., Michiels, C. W., & Nilsen, I. W. (2013). Enzyme characterisation and gene expression profiling of Atlantic salmon chicken- and goose-type lysozymes. *Developmental and Comparative Immunology, 40*(1), 11–19. https://doi.org/10.1016/j.dci.2013.01.010

Naka, T., Nishimoto, N., & Kishimoto, T. (2002). The paradigm of IL-6: From basic science to medicine. *Arthritis Research, 4*, 1–10. https://doi.org/10.1186/ar565

Pacheco, F. J., Pacheco, S. O. S., Segreto, H. R. C., Segreto, R. A., Silva, M. R. R., & Egami, M. I. (2002). Development of granulocytes in haematopoietic tissues of *Rhizoprionodon lalandii*. *Journal of Fish Biology, 61*(4), 888–898. https://doi.org/10.1111/j.1095-8649.2002.tb01850.x

Pérez-Cordón, G., Estensoro, I., Benedito-Palos, L., Calduch-Giner, J. A., Sitjà-Bobadilla, A., & Pérez-Sánchez, J. (2014). Interleukin gene expression is strongly

modulated at the local level in a fish–parasite model. *Fish & Shellfish Immunology, 37* (2), 201–208. https://doi.org/10.1016/j.fsi.2014.01.022

Petrie-Hanson, L., & Peterman, A. E. (2005). American paddlefish leukocytes demonstrate mammalian-like cytochemical staining characteristics in lymphoid tissues. *Journal of Fish Biology, 66*(4), 1101–1115. https://doi.org/10.1111/j.0022-1112.2005.00668.x

Reite, O. B. (1972). Comparative physiology of histamine. *Physiological Reviews, 52*(3), 778–819. https://doi.org/10.1152/physrev.1972.52.3.778

Sayyaf Dezfuli, B., Castaldelli, G., Lorenzoni, M., Carosi, A., Ovcharenko, M., & Bosi, G. (2023a). Rodlet cells provide first line of defense against swimbladder nematode and intestinal coccidian in *Anguilla anguilla*. *Fishes, 8*(2), 66. https://doi.org/10.3390/fishes8020066

Sayyaf Dezfuli, B., Giari, L., & Bosi, G. (2021). Survival of metazoan parasites in fish: Putting into context the protective immune responses of teleost fish. *Advances in Parasitology, 112*, 77–132. https://doi.org/10.1016/bs.apar.2021.03.001

Sayyaf Dezfuli, B., Lorenzoni, M., Carosi, A., Giari, L., & Bosi, G. (2023b). Teleost innate immunity, an intricate game between immune cells and parasites of fish organs: Who wins, who loses. *Frontiers in Immunology, 14*, Article 1250835. https://doi.org/10.3389/fimmu.2023.1250835

Sayyaf Dezfuli, B., Manera, M., Bosi, G., Merella, P., DePasquale, J. A., & Giari, L. (2018a). Intestinal granular cells of a cartilaginous fish, thornback ray *Raja clavata*: Morphological characterization and expression of different molecules. *Fish & Shellfish Immunology, 75*, 172–180. https://doi.org/10.1016/j.fsi.2018.02.019

Sayyaf Dezfuli, B., Giari, L., Lorenzoni, M., Carosi, A., Manera, M., & Bosi, G. (2018b). Pike intestinal reaction to *Acanthocephalus lucii* (Acanthocephala): Immunohistochemical and ultrastructural surveys. *Parasites & Vectors, 11*, 1–12. https://doi.org/10.1186/s13071-018-3002-6

Sayyaf Dezfuli, B., Manera, M., Bosi, G., Merella, P., DePasquale, J. A., & Giari, L. (2019). Description of epithelial granular cell in catshark spiral intestine: Immunohistochemistry and ultrastructure. *Journal of Morphology, 280*(2), 205–213. https://doi.org/10.1002/jmor.20932

Schridde, A., Bain, C. C., Mayer, J. U., Montgomery, J., Pollet, E., Denecke, B., Milling, S. W. F., Jenkins, S. J., Dalod, M., Henri, S., Malissen, B., Pabst, O., & Mcl Mowat, A. (2017). Tissue-specific differentiation of colonic macrophages requires TGFβ receptor-mediated signaling. *Mucosal Immunology, 10*(6), 1387–1399. https://doi.org/10.1038/mi.2016.142

Seno, H., Sawada, M., Fukuzawa, H., Morita-Fujisawa, Y., Takaishi, S., Hiai, H., & Chiba, T. (2002). Involvement of Tumor Necrosis Factor Alpha in intestinal epithelial cell proliferation following Paneth cell destruction. *Scandinavian Journal of Gastroenterology, 37*(2), 154–160. https://doi.org/10.1080/003655202753416803

Shaw, T. N., Houston, S. A., Wemyss, K., Bridgeman, H. M., Barbera, T. A., Zangerle-Murray, T., Strangward, P., Ridley, A. J. L., Wang, P., Tamoutounour, S., Allen, J. E., Konkel, J. E., & Grainger, J. R. (2018). Tissue-resident macrophages in the intestine are long lived and defined by Tim-4 and CD4 expression. *Journal of Experimental Medicine, 215*(6), 1507–1518. https://doi.org/10.1084/jem.20180019

Smith, N. C., Rise, M. L., & Christian, S. L. (2019). A comparison of the innate and adaptive immune systems in cartilaginous fish, ray-finned fish, and lobe-finned fish. *Frontiers in Immunology, 10*, Article 475871. https://doi.org/10.3389/fimmu.2019.02292

Sudhagar, A., El-Matbouli, M., & Kumar, G. (2020). Identification and expression profiling of Toll-Like Receptors of Brown trout (*Salmo trutta*) during proliferative kidney disease (PKD). *International Journal of Molecular Sciences, 21*(11), 3755. https://doi.org/10.3390/ijms21113755

Webster, J. D., Solon, M., & Gibson-Corley, K. N. (2021). Validating immunohistochemistry assay specificity in investigative studies: Considerations for a weight of evidence approach. *Veterinary Pathology, 58*(5), 829–840. https://doi.org/10.1177/0300985820960132

Zapata, A., & Amemiya, C. T. (2000). Phylogeny of lower vertebrates and their immunological structures. In L. Du Pasquier, & G. W. Litman (Eds.), *Origin and evolution of the vertebrate immune system, current topics in microbiology and immunology* (pp. 67–107). Springer. https://doi.org/10.1007/978-3-642-59674-2_5.

Zapata, A. G., Torroba, M., Sacedón, R., Varas, A., & Vicente, A. (1996). Structure of the lymphoid organs of elasmobranchs. *The Journal of Experimental Zoology Part a: Ecological Genetics and Physiology, 275*(2–3), 125–143. https://doi.org/10.1002/(SICI)1097-010X(19960601/15)275:2/3<125::AID-JEZ6>3.0.CO;2-F

Zhang, J., Kong, X., Zhou, C., Li, L., Nie, G., & Li, X. (2014). Toll-like receptor recognition of bacteria in fish: Ligand specificity and signal pathways. *Fish & Shellfish Immunology, 41*(2), 380–388. https://doi.org/10.1016/j.fsi.2014.09.022

Zou, J., & Secombes, C. (2016). The function of fish cytokines. *Biology, 5*(2), 23. https://doi.org/10.3390/biology5020023